CONSERVAR PATRIMÓNIO

in Press **ARTICLE / ARTIGO**

Non-invasive pXRF technique for identifying pigments in multilayered artistic paintings

pXRF: técnica não invasiva para identificar pigmentos em pinturas artísticas com multicamadas

ROSARIO BLANC
ELOISA MANZANO*
JOSÉ LUIS VÍLCHEZ

Research Group of Analytical Chemistry and Life Sciences, Department of Analytical Chemistry, Faculty of Sciences, University of Granada, Avda. Fuentenueva s/n, 18071 Granada, Spain

emanzano@ugr.es

Abstract

Portable X-ray fluorescence (pXRF) is a powerful analytical tool; however, its application to the analysis of complex pigment mixtures and multilayered artistic paintings – particularly ternary and quaternary systems distributed across one or more layers – still presents significant challenges. This study investigates the effectiveness of pXRF in detecting specific pigments, such as azurite, cinnabar, and lead white, within complex mixtures and overlapping stratigraphic layers, which are typical features of historical paintings and polychrome sculptures. Cadmium yellow, a pigment commonly used in later periods as overpainting, was also successfully identified, providing insights into the usefulness of pXRF for testing on historical artworks, even when dealing with later additions or restorations. The insights gained from these experimental replicas were subsequently applied to the analysis of two historical paintings selected as case studies, in which the target pigments were found to be heterogeneously distributed and mixed in varying proportions.

KEYWORDS
pXRF
Multi-layered model sample
Cinnabar
Azurite
Cadmium yellow
Lead white

Resumo

A fluorescência de raios X portátil (pXRF) é uma ferramenta analítica poderosa; no entanto, a sua aplicação na análise de misturas complexas de pigmentos e pinturas artísticas com várias camadas – particularmente sistemas ternários e quaternários distribuídos por uma ou mais camadas – ainda apresenta desafios significativos. Este estudo investiga a eficácia da pXRF na deteção de pigmentos específicos, como azurite, vermelhão e branco de chumbo, em misturas complexas e camadas estratigráficas sobrepostas, comum em pinturas históricas e esculturas policromáticas. O amarelo de cádmio, um pigmento muito usado em períodos posteriores como sobrepintura, também foi identificado, mostrando a utilidade do pXRF para analisar obras de arte históricas, mesmo quando se trata de adições ou restauros posteriores. As informações obtidas com as réplicas experimentais foram posteriormente usadas para analisar duas pinturas históricas selecionadas como casos de estudo. Os pigmentos identificados estão distribuídos de forma heterogénea e misturados em proporções variadas.

PALAVRAS-CHAVE
XRF portátil
Amostra padrão em multicamadas
Cinábrio
Azurite
Amarelo cádmio
Branco de chumbo

Introduction

Art scientists play a crucial role in the multidisciplinary study of cultural heritage (CH), developing modern techniques and innovative strategies to investigate historical and artistic materials. Multidisciplinary research can yield valuable insights into artistic heritage by combining expertise from heritage sciences. The investigative focus has shifted in recent years towards non-invasive, in situ methods, so the need has arisen for portable instruments for in-field assessments. One analytical technique widely cited in the literature is energy dispersive X-ray fluorescence (XRF) spectrometry, which has been used for elemental characterisation since the 1960s [1-8]. This is now widely and successfully used to provide non-destructive elemental analysis of pigments on polychrome surfaces, easel paintings, historical manuscripts, and even in archaeological and forensic applications [7, 9-16]. The use of portable X-ray fluorescence (p-XRF) spectrometry for in situ multi-elemental analysis has grown exponentially, but some limitations have been noted. These include its low sensitivity in detecting light elements, the over-lapping or proximity of some X-ray lines, such as the SKα line and PbMα lines [17-18], and the influence on the fluorescence signal of the elements of the sample matrix. This last effect plays a crucial role in the detection of pigments using pXRF because it can either enhance or attenuate the fluorescence signal of the heaviest element of a pigment, depending on the surrounding materials and their composition [19].

The X-rays are attenuated because in the fluorescence process they are generated both in the atoms on the surface of the sample and in those within the sample. When a beam of X-ray photons passes through a material, some photons are attenuated in the interaction processes, following the Beer-Lambert law. The intensity of both the incident X-ray beam and the fluorescent radiation is reduced due to absorption in the sample; the degree of reduction depends on the density, thickness, and mass attenuation coefficient of all the elements in the matrix. This variability can make it challenging to identify these elements accurately, which is particularly relevant to attempts to understand the materials and techniques used by artists in the field of art conservation and restoration. Several recent studies have examined the factors involved in the in situ pXRF analysis of pigments, particularly from complex layered samples. Literature has focused on layer thickness, pigment dilution in the binder (critical Pigment Volume Concentration or PVC), pigment particle size, layer homogeneity, and the matrix effect, particularly on the complex stratigraphic structures of paintings and their influence on the measurement of the fluorescence signal [8-9, 20-23].

Progress has been made, such as in the visualisation of the distribution of elements within complex structures through macro XRF mapping, the variation of the angle of X-ray incidence (angular scanning) [19, 21], and the evaluation of layer stratigraphic disposition and measurement of its thickness through the Monte Carlo (MC) algorithm, and the use of X-ray intensity ratios (such as Kα/Kβ or Lα/Lβ) [2, 8, 24-28]. However, despite ongoing investigation, the matrix effect of elements from different pigments within the pictorial medium remains a challenging topic in the case of polychromatic multilayers and complex pigment mixtures such as easel paintings. This topic is the focus of the present study.

The present work is one element of our multidisciplinary research, which aims to develop advanced non-invasive techniques to extract the maximum possible information from artistic paintings. In particular, an interesting line of research in our project focuses on studying pigment mixtures in real paintings signed by renowned artists [2, 26, 29]. Our current research delves deeper into this topic, mainly addressing questions related to the analysis of complex multilayers and mixtures in unknown painting samples by pXRF spectrometry. Our main goal is to establish the reliability of this technique for detecting the component elements of pigments, even in binary, ternary, and quaternary mixtures of pigments. The pigments are spread pure or mixed (2, 3 or 4 pigments) in single or multilayered pictorial structures. Given the mixtures of pigments traditionally used, we selected cinnabar, azurite, and cadmium yellow, in both pure and mixed forms [30]. The combination of these pigments in various ways

reflects the techniques traditionally used to achieve a wide range of colours and effects in artworks. Small amounts of cinnabar and azurite mixed in the flesh tones of living figures are common in traditional paintings and sculptures, while azurite combined with red pigment and lead white produces purple tones, and with cadmium yellow forms green. Lead white – widely used as *imprimatura* or for light areas in many artistic paintings in the past – was also chosen to study its influence in different mixtures. Finally, findings from the experimental replica samples studied are applicated to two real paintings used as case study.

Materials and methods

Pigments and binder medium

The selected pigments – cinnabar, azurite, cadmium yellow, and lead white – were used in their pure form and as mixtures, with refined linseed oil (Winsor & Newton) as the pigment binder in all the model samples. The pigments azurite (Standard PB 30 (A), $Cu_3(CO_3)_2(OH)_2$, 10200 code Kremer), lead white (LW, $(PbCO_3)_2{\cdot}Pb(OH)_2$, 46000 code Kremer) and cinnabar (C, HgS, 42000 code Kremer) were used for centuries in European easel painting, particularly during the fifteenth and sixteenth centuries. Additionally, a more recent pigment developed in the nineteenth century, cadmium yellow (CY, CdS, 21040 code Kremer), was included in this study. The CdS pigment used in this study is consistent with historical CdS–CdZnS formulations employed to lighten cadmium yellow tones. The Zn content remains below the detection limit of our analytical methods. The reason for including an anachronistic pigment in this study lies in its potential presence, possibly added during a repainting or retouching as part of a restoration process. This pigment introduces a new element (Cd) with different spectral lines compared to the previous pigments (Pb, Cu, Hg), providing insights into the usefulness of pXRF for testing on historical artworks, even when dealing with later additions or restorations.

Model paint samples

Test panels were prepared in the laboratory on one canvas support; each panel replicates a layered artistic painting. Twenty-four model samples were prepared, containing both pure pigments (cinnabar, azurite, cadmium yellow and lead white) and mixtures of these, arranged in one, two or three layers. The successive layers were applied with a brush. All pigments were manually mixed in a porcelain glass for a few minutes, using a glass rod, with linseed oil as the medium. The amount of linseed oil used simulated the standard proportions of pigment mixtures, which must have an optimal consistency, not drip during application, and achieve a homogeneous layer. The amount of oil absorbed by each pigment varies due to pigment grain size, form, and chemical composition, but the optimal pigment/linseed oil (w/w) ratio required to obtain an appropriate viscosity of paint for each pigment studied was 3:1 (1.5 g of pigment to 0.5 ml of linseed oil). This ratio was maintained in the mixtures. The structure was designed to reproduce a paint layer thickness typical of real paintings, reaching approximately 100 µm, measured using a Mitutoyo 2046F thickness gauge (measurement range: 0.01-10 mm). Each layer was applied and then allowed to dry under controlled laboratory conditions (22 °C, 50 % RH) without direct exposure to light. After approximately 72 hours, when the layer had fully dried to the touch, the subsequent layer was applied on top of the previous one. The study was carried out using a portable XRF spectrometer. For each model sample, three measurement points were considered, and the calculated signal fluorescence was averaged from the number of counts per second of the three measurements taken with a precision of 1.43 %. The indicated precision was evaluated as the percentage ratio between semi-dispersion error and averaged value. One hundred and twenty-nine measurements were carried out in this way with pXRF, including support measurements.

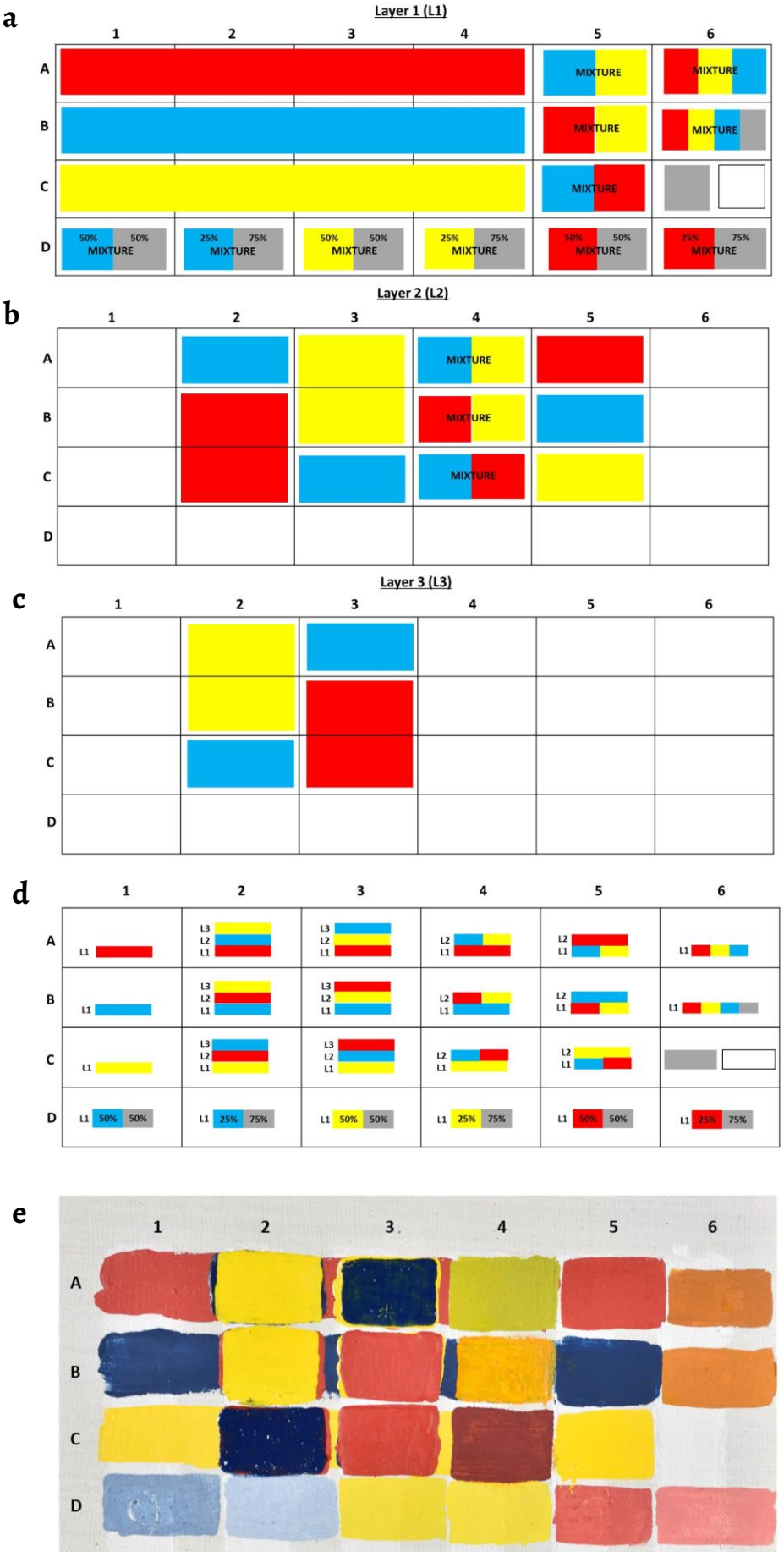

Figure 1. Schematic structure of the model samples: *a)* in the first layer; *b)* second layer; c) third layer; *d)* the outline of its stratigraphic layout and *e)* the final state of the model sample. Red – HgS, blue - $Cu_3(CO_3)_2(OH)_2$, yellow – CdS, grey – $(PbCO_3)_2{\cdot}Pb(OH)_2$ and white – canvas. The size of each cell is 2.5 × 5 cm.

Figure 1 schematises the stratigraphic arrangement of the pure and mixed pigments in the first (Figure 1a), second (Figure 1b), and third layers (Figure 1c) of the model samples. Figure 1 shows how the first layer (L1) was prepared with pure pigments (cinnabar 1-4A; azurite 1-4B; cadmium yellow 1-4C and lead white 6C) and binary, ternary and quaternary mixtures of pigments. Binary mixtures were prepared with combinations of two of cinnabar, azurite, and cadmium yellow pigments in a 1:1 ratio (5A-C) and combinations of one of these pigments with white lead at 1:1 and 3:1 ratio (1-6D). A ternary mixture sample of cinnabar, azurite, and cadmium yellow in equal proportions was prepared (6A), and a quaternary mixture sample was prepared, composed of the three previous pigments plus lead white, also in equal proportions (6B). The second layer (L2) was prepared on top of the first. Pure pigments (2A-C, 3A-C and 5A-C) and binary mixtures (4A-C) were spread on top of the first layer. The third layer (L3) was prepared on top of the second layer with pure pigments (2A-C and 3A-C). In addition, the stratigraphic structure of the model samples is shown, where the inner layer is L1, the middle layer L2 and the outer layer L3 (Figure 1d). Finally, the photograph of the final state of the model samples is shown (Figure 1e).

Case study: description of the paintings

To support our experimental testing with replica samples, two paintings were selected (case study No. 1 and No. 2) for study. The artworks were attributed to the sixteenth century and feature the use of lead white, vermilion or cinnabar, and azurite pigments in their layers. Both paintings belong to a private collection and were studied by our research group. In each artwork, specific color areas (red, blue, and flesh tones) were selected for analysis, which contain some of the pigment mixtures discussed in the study (Figure 2).

Figure 2. The case study paintings: *a)* No. 1, painting on copper support; *b)* No. 2, painting on canvas: *The Little Madonna of Foligno*.

Case study No. 1 comprises an oil painting on a copper support, on the back of which is the inscription, *Boceto di Pablo Veronese*. The painting (Figure 2a) is oval shaped with two axes of symmetry (major axis: 17.5 cm; minor axis: 13.5 cm). The theme of the painting is religious, representing the Holy Family [2].

Case study No. 2 is an oil painting entitled *The Little Madonna of Foligno*, dated between 1507 and 1509. It depicts a scene almost identical to that of Raphael Sanzio's Madonna of Foligno from the Italian High Renaissance (around 1511), which is displayed in the Vatican Pinacoteca (Figure 2b). The *Little Madonna of Foligno* is smaller (66.5 × 93.5 cm) and includes additional details, such as the almost complete head of a lion behind Sigismund of Conti's cape [29].

Handheld X-ray fluorescence (pXRF)

X-ray fluorescence spectroscopy analysis was performed using a handheld NITON XL3t GOLDD+ (Thermo Fisher Scientific, Waltham, MA, USA) with a silver anode (50 kV, 200 A) analyser (pXRF). The analyser was fitted with a camera and a suitably equipped Small Spot analyser, with which analysis could be restricted to a small area of the camera angle (3 mm). After waiting five minutes to allow the instrument's electronics to stabilize, a system check was performed to calibrate the detector and ensure it was operating according to the specifications. Spectra were collected using the measuring mode "test all geo". The analyser was equipped with four excitation filters (main, high, low, and light) that optimise the analyser's sensitivity for the various elements. Measurements of 30 seconds for each filter were set, meaning each spot analysis took approximately 120 seconds to complete. The geometrical setup was the same for all the measurements. NITON Data Transfer (NDT) software 6.1 was used to control the instrument and for management and transfer.

Results

The results of the pXRF measurements of the model pictorial samples, with the pigments used in pure form, mixed, or layered, are shown below. This was followed by a discussion on the influence on the fluorescence signal of the presence of other pigments in mixtures and/or in multiple layers. The current section begins with the description of the XRF results for model samples when the analysed pigment is pure and located in the outer, inner or middle layer. The following section deals with the results obtained on the pigment mixtures, as either external or internal layers. Finally, the results obtained in the study of laboratory samples were supported using pXRF to identify these pigment mixtures in two real paintings.

For the present study, the number of counts per second (cps) of the spectral lines of the heaviest element of each pigment – HgLα for cinnabar, CuKα for azurite, CdKα for cadmium yellow and PbLα for lead white – was measured. Bar charts are used to plot the mean values of various elements (Hg, Cu, Cd, Pb) from three random measurements. These measurements are taken when the pigment analysed is located in the outermost, innermost, or middle layer of a model sample with one, two, or three layers. The elements found in the canvas support (majority Zn and traces of Ba, Pb, Fe, S and Ca) do not affect the results obtained.

Model samples of pure pigments

Representative pXRF spectra of pure pigments measured in a mono layer were selected for display in Figure 3. The figure displays the characteristic spectral lines of the chemical elements in each pigment and illustrate how each pigment can be differentiated.

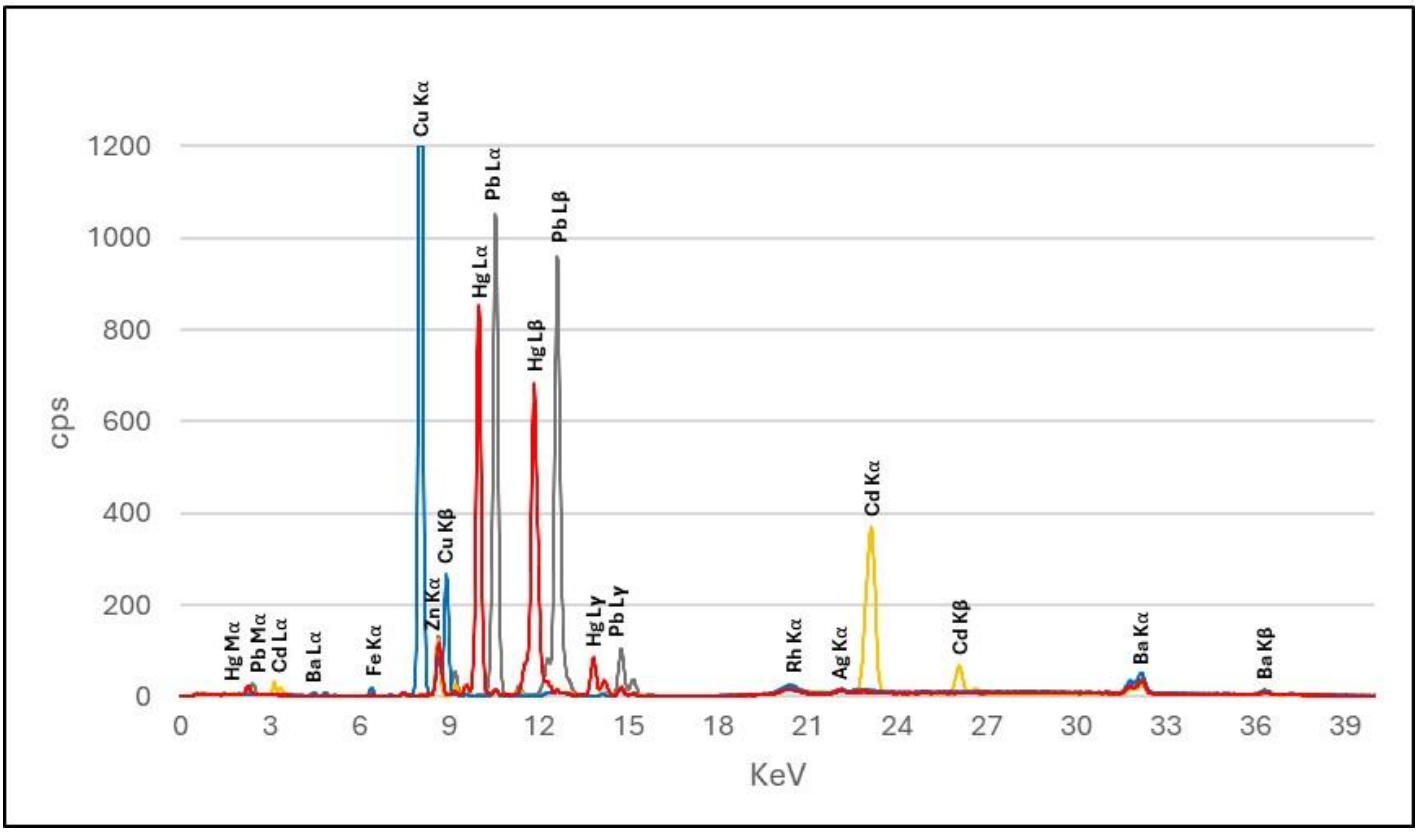

Figure 3. pXRF spectra of pure pigments: red - HgS, blue - $Cu_3(CO_3)_2(OH)_2$, yellow - CdS, grey - $(PbCO_3)_2{\cdot}Pb(OH)_2$.

Pure pigment in the outermost layer

When the pure cinnabar, azurite or cadmium yellow was situated in the outermost layer, the counts per second (cps) of the peak of the heaviest element in a mono layer (L1) was compared with its signal when measured over two- (L2) or three-layered (L3) model samples.

Figure 4a shows a decrease in the X-ray fluorescence signal of the HgLα line of a pure cinnabar when it is extended over a layer of azurite or cadmium yellow (30 % to 47 %, respectively). It should be noted that when there was two layers of pigment under the cinnabar, the X-ray fluorescence signal HgLα was unaffected. Note also that the order of the two pigments under the cinnabar layer did not affect the HgLα signal.

If pure azurite was the outermost layer (Figure 4d), the bar chart showed a prominent CuKα line, but this was reduced by about 50 % when the cinnabar was present in internal layers. However, only a slight reduction in the CuKα line (around 15 %) was observed when cadmium yellow is the underlying pigment.

The X-ray fluorescence intensity of the CdKα line from pure cadmium yellow in a mono layer (Figure 4g) was significantly less than the CuKα and HgLα lines in the same disposition. However, it should be noted that its signal increased by 40-50 % when the yellow pigment was spread in the outer layer of a bilayer sample. This signal increased was only observed in bilayer samples; it did not occur in trilayer samples.

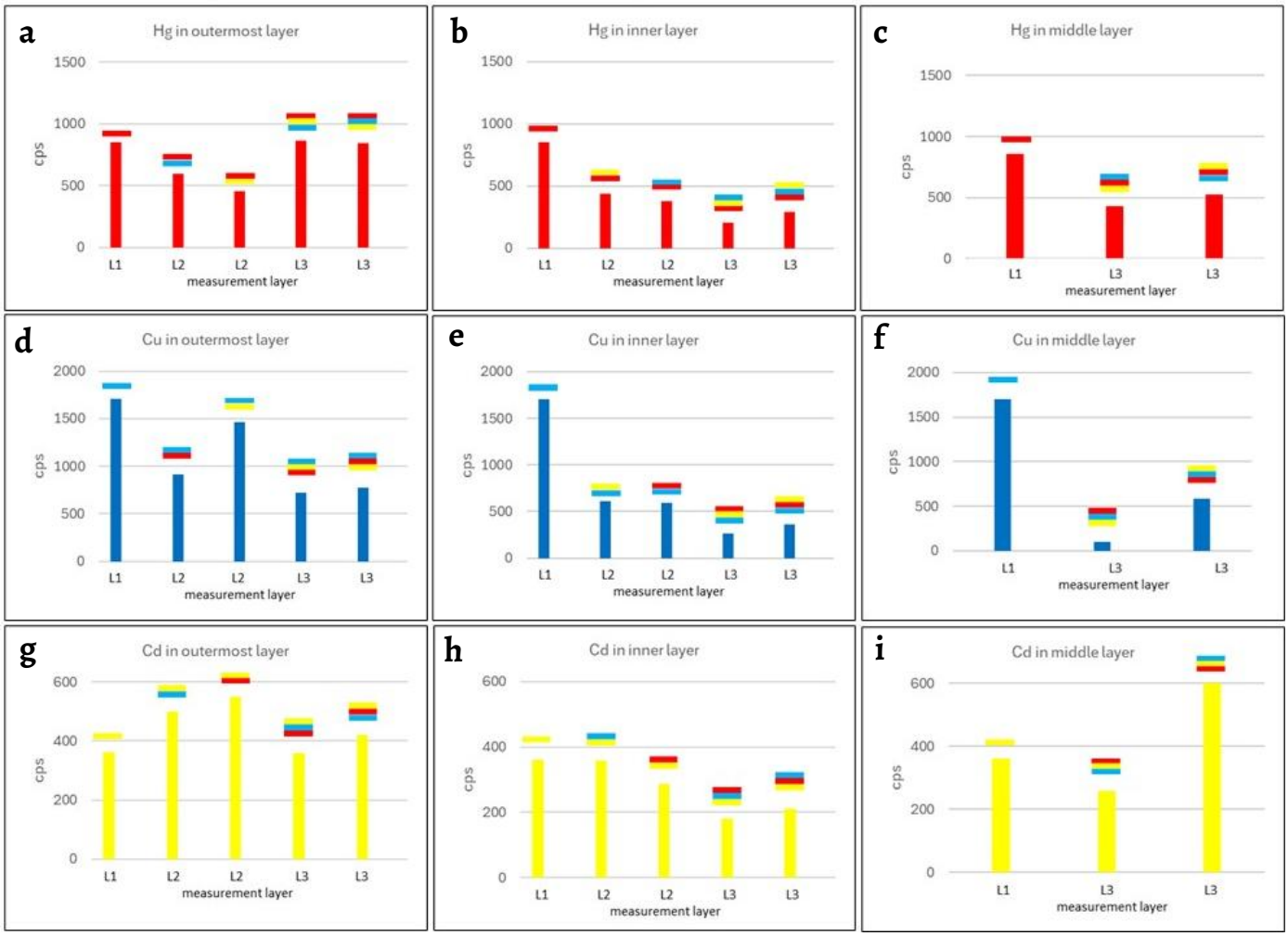

Figure 4. Counts per second (cps) of the peak of: *a-c)* HgLα; *d-f)* CuKα; *g-i)* CdKα, for each pure pigment when measured in the outermost, inner and middle layer. Red - HgS, blue - $Cu_3(CO_3)_2(OH)_2$, yellow - CdS. The small colored segments at the top of each bar illustrate the pigment stratigraphy corresponding to the successive layers, as documented in Figure 1.

Pure pigment in middle and inner layers

When cinnabar or azurite pigments were in the inner or middle layers of two- or three-layer samples, a significant reduction was observed in the X-ray fluorescence signal of HgLα or CuKα, compared to that in the single pigment. This observed reduction was independent of the number of paint layers and the location of the pigment being measured (L1, L2 or L3) (Figure 4b-c, e-f). Notably, there was a significant reduction of the CuKα fluorescence signal (90 %) when azurite was in the middle layer under an outer layer of cinnabar. The presence of an outer layer of cinnabar significantly affected the copper signal of the blue pigment located in the lower layer. The CdKα signal, though, was barely affected by the presence of cinnabar, although a notable increase in its signal was observed in three-layer samples with azurite in the outermost layer.

Model samples of mixed pigments

In order to study the influence of the pigment mixture on the fluorescence signal of the pictorial matrix, fourteen model samples were prepared, including single- and two-layer samples (Figure 1). Figure 5 shows selected pXRF spectra of samples of mixed pigments.

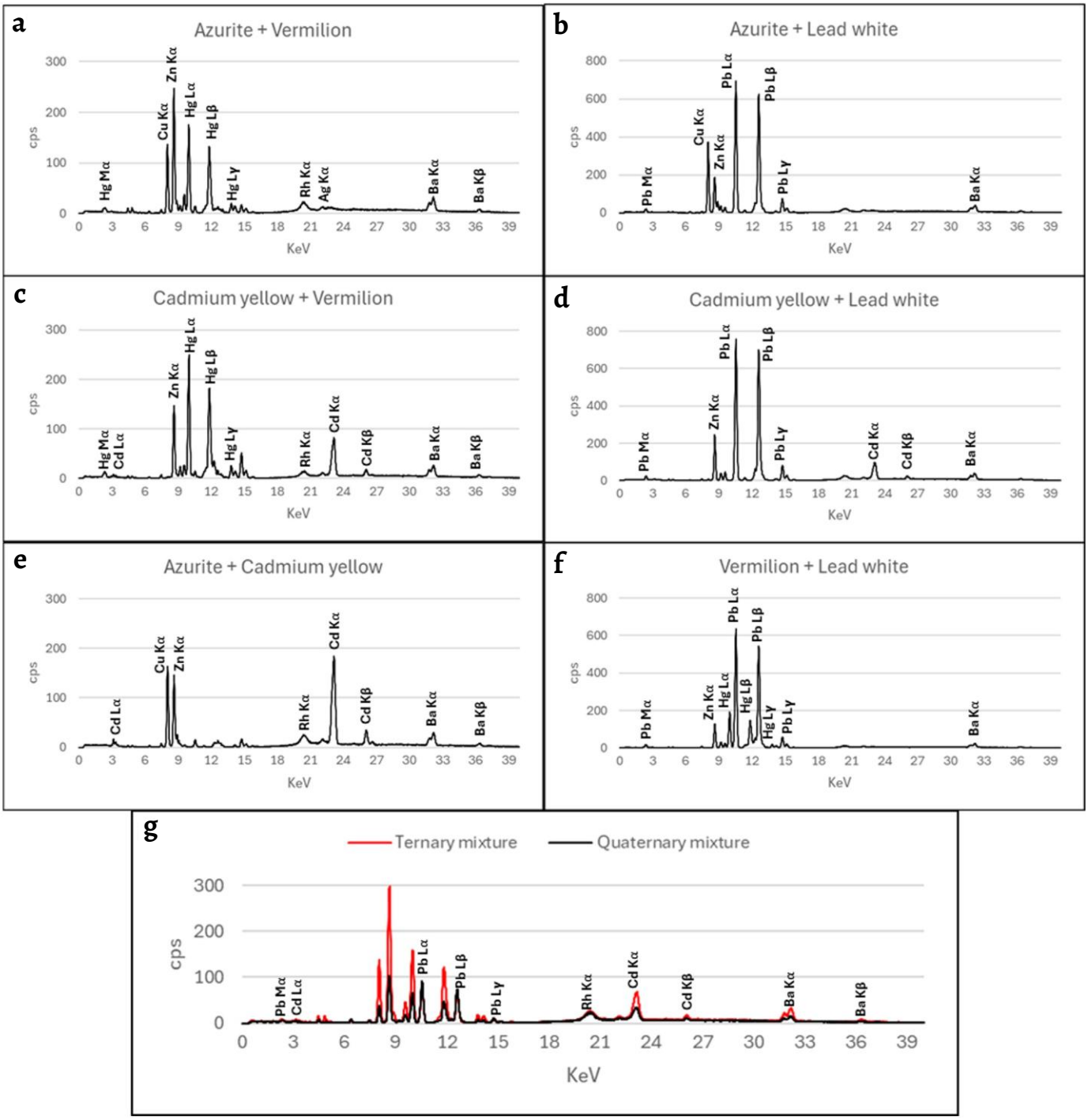

Figure 5. pXRF spectra of model samples of binary, ternary and quaternary mixtures with equal proportions of pigments: *a)* binary mixture of azurite and cinnabar; *b)* binary mixture of azurite and lead white; *c)* binary mixture of cadmium yellow and cinnabar; *d)* binary mixture of cadmium yellow and lead white; *e)* binary mixture of azurite and cadmium yellow; *f)* binary mixture of cinnabar and lead white and *g)* red-ternary mixture (azurite, cinnabar and cadmium yellow) and black-quaternary mixture (azurite, cinnabar, cadmium yellow and lead white).

Mix pigments in the external layer

This section focuses on 11 model samples containing pigment mixtures in the outermost layer. In eight of them, the mixtures were spread in a single layer, and in the other three, the mixtures were in the outer layer of two-layer samples (Figure 1). The single-layer samples contained binary, ternary, and quaternary mixtures, with equal pigment proportions (1:1, 1:1:1, and 1:1:1:1 ratios), and binary mixtures of lead white and pigment with a 1:1 (LW:pigment) and a 3:1 (LW:pigment) ratio (Figure 1).

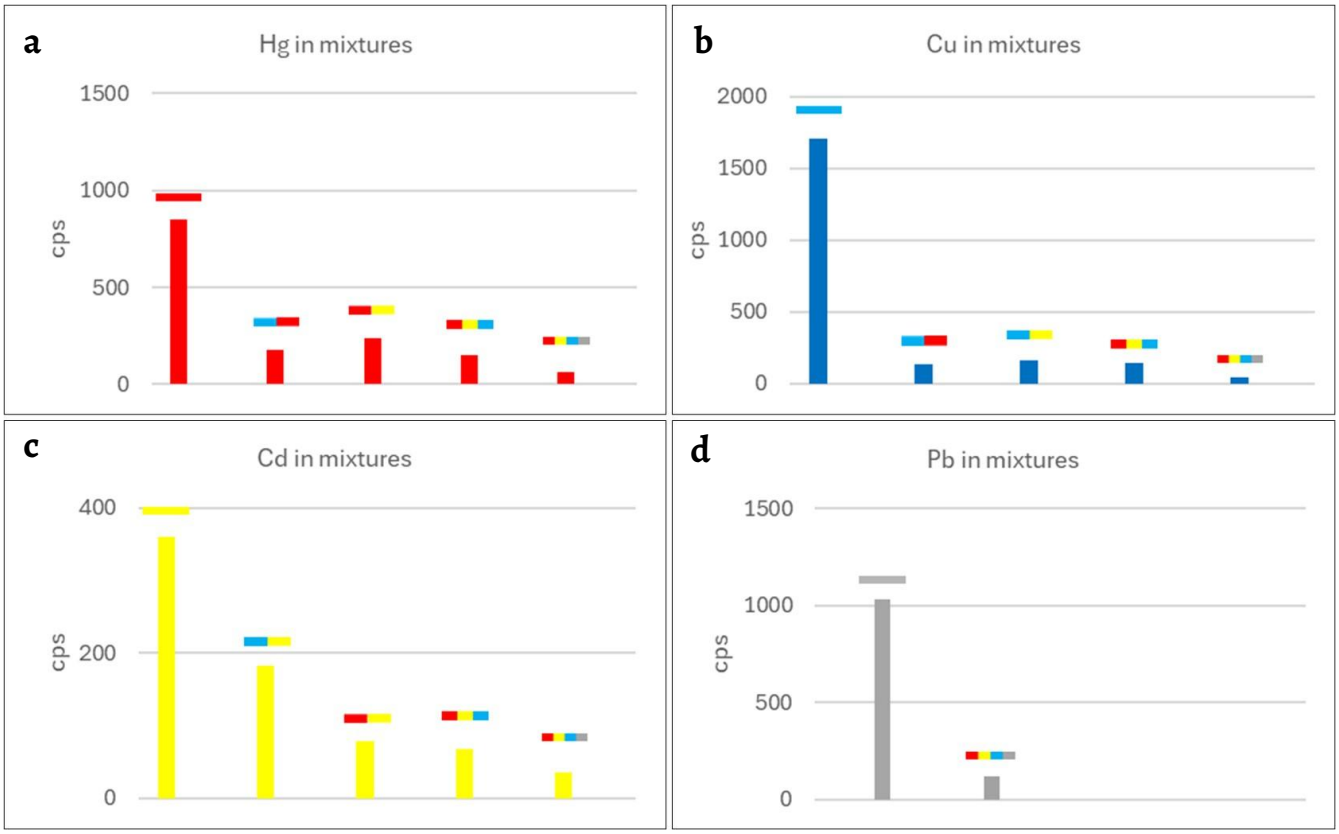

Figure 6. Counts per second (cps) of the peak of: 1*a)* HgLα; 1*b)* CuKα; 2*c)* CdKα; 2*d)* PbLα for each mixture. Red - HgS, blue - $Cu_3(CO_3)_2(OH)_2$, yellow - CdS, grey - $(PbCO_3)_2{\cdot}Pb(OH)_2$.

The bar charts in Figure 6 show that all the pigments measured show a much lower fluorescence signal than the pure pigment signal when they were part of a binary, ternary, or quaternary mixture. The decrease was greater than 50 % in all tested mixtures. This occurs particularly in the quaternary mixture, where the HgLα, CuKα, CdKα, and PbLα signals were reduced by up to 95 %.

Figure 7 illustrates the impact of lead white (LW: pigment) on the X-ray fluorescence signals of other pigments in binary mixtures. The presence of Pb in mixtures significantly reduced the X-ray fluorescence signals of other pigments, the HgLα, CuKα, and CdKα signals at a 1:1 ratio with Pb were up to 80 % lower than the signal of the pure pigment. The reduction of the measured X-ray fluorescence signal of PbLα in the three binary mixtures was lower, however, in particular for LW:CY (3:1) and for LW:A (3:1). When the proportion of azurite in the mixture was increased (1:1 ratio), the PbLα signal was reduced by around 40 %. Mixtures with cinnabar showed the most significant reduction in the X-ray fluorescence measurement of Pb, even when lead white constituted 75 % of the mixture.

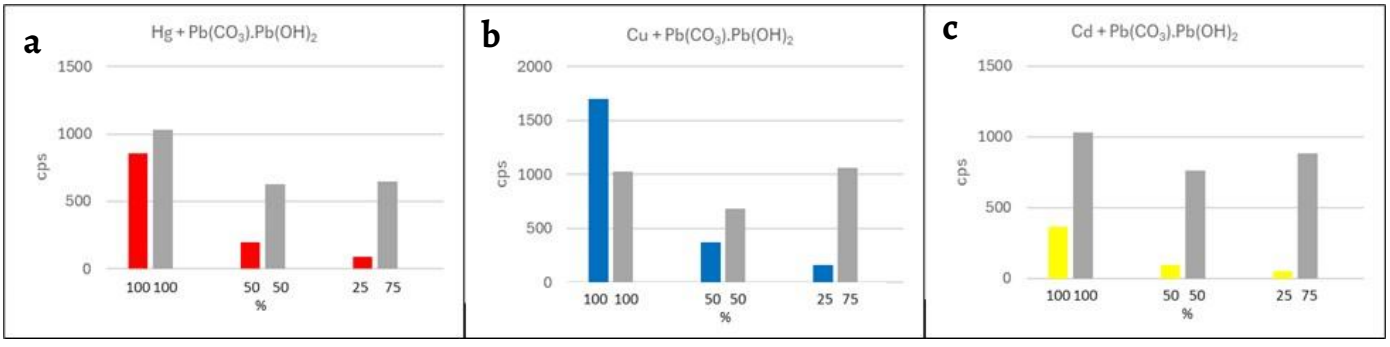

Figure 7. Counts per second (cps) of the peak of HgLα, CuKα, CdKα or PbLα for binary mixtures between different pigments and lead white in a single layer: *a)* binary mixture of cinnabar and lead white; *b)* binary mixture of azurite and lead white and *c)* binary mixture of cadmium yellow and lead white. Red - HgS, blue - $Cu_3(CO_3)_2(OH)_2$, yellow - CdS, grey - $(PbCO_3)_2{\cdot}Pb(OH)_2$.

Finally, this section studies how the mixture of pigments affects the X-ray fluorescence signal when this mixture was in the outer layer of a two-layer sample (Figure 1d, 4A-C). The results are shown in the bar charts of Figure 8a, c and, e.

When pure pigments were spread on the outer layer over a mixture, there was very little reduction in the HgLα and CdKα fluorescence signal, but the azurite signal was reduced by almost 45 %. However, the decrease in the signal was significant if the measured pigment was on the outer layer but in a mixture; the HgLα signal, especially, was drastically attenuated – by 90 % – despite being in the outer layer.

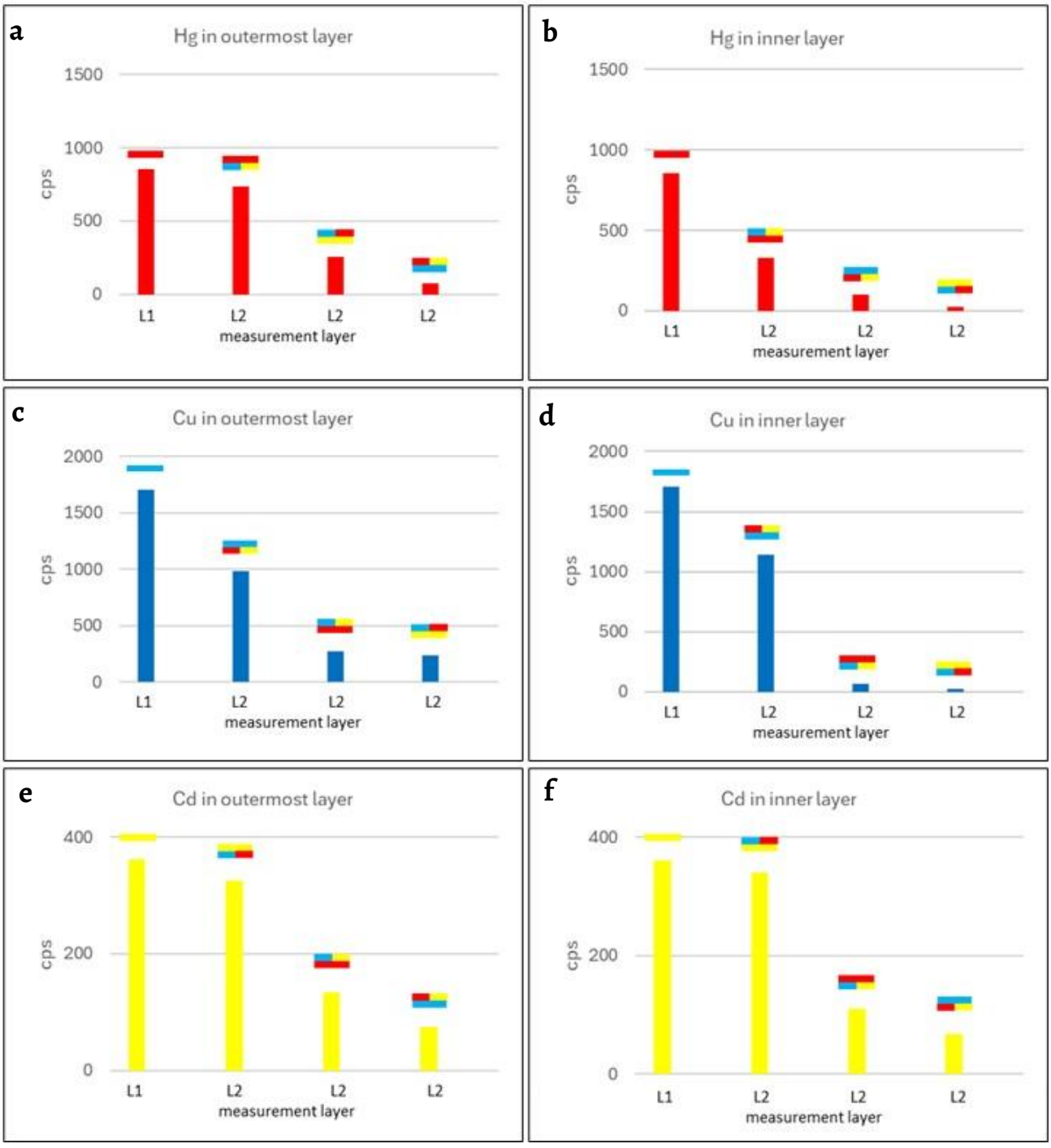

Figure 8. Counts per second (cps) of the peak of: *a-b)* HgLα; *c-d)* CuKα; and *e-f)* CdKα in outermost and inner layers for pigment mixtures spread on two-layer samples. Red - HgS, blue - $Cu_3(CO_3)_2(OH)_2$, yellow - CdS. The small colored segments at the top of each bar illustrate the pigment stratigraphy and mixtures corresponding to the successive layers, as documented in Figure 1.

Mix pigments in the inner layer

The X-ray fluorescence signal of pure or mixed pigments located in the inner layer was shown in the bar charts of Figure 8b, d and, f. When the pigment being measured was pure under a mixture layer, the HgLα signal is reduced by 60 % and the CuKα signal by 30 %. In contrast, the signal of pure cadmium yellow remains constant. However, when the pigment being measured was mixed and located in the inner layer, the reduction in HgLα and CuKα signals was more significant than when the pigment was is pure. The CdKα signal was only affected if the pigment was mixed, and it was unaffected by whether it was in the inner or outer layer.

Stratigraphical information obtained by measuring the intensity of different spectral lines by pXRF

The spectrum of pXRF measurements of the model pictorial samples showed different spectral lines depending on whether the pigment is in an external or internal layer. As indicated in the bibliography consulted "the energetic emission from the PbLα line (10.3 keV), being poorly attenuated, is related to the presence of lead elements in the whole stratigraphy. On the other hand, the detected emission from the PbMα line (2.38 keV) is related to surface layers only, since photons emitted in underlying layers are strongly absorbed by upper layers" [31-32].

As shown in Figure 3 and Figure 5, the lead white was in an external layer in all the model samples in our study. Therefore, in the corresponding spectrum, we observe the spectral lines of PbLα and PbMα.

Figure 9 shows the same situation for cinnabar and cadmium yellow, respectively. If both pigments were in external layers, the peaks corresponding to the spectral lines HgMα and CdLα appear, and if they were in internal layers, they did not appear. This phenomenon was independent of whether the pigments were pure or mixed.

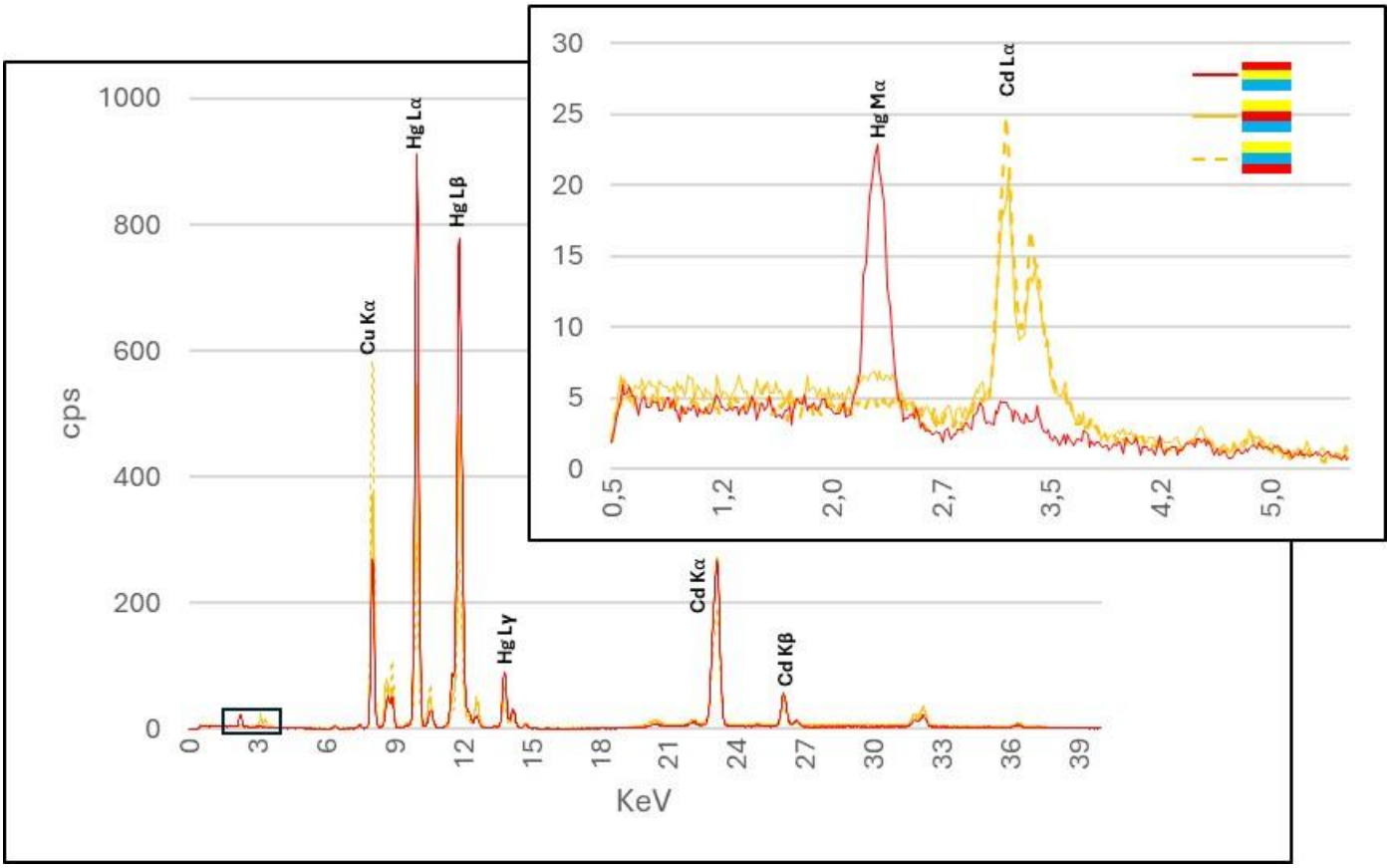

Figure 9. pXRF Spectra of model samples with cinnabar or cadmium yellow in the surface layer. red HgS, blue $Cu_3(CO_3)_2(OH)_2$, yellow CdS.

Two case studies: results

Two artworks (case study No.1 and No.2) have been analysed previously by our research group [2, 29], in situ, using pPXRF and XRD so they were used to reinforce the laboratory data and support the pXRF findings. In each painting, specific colour areas were selected for analysis, containing some of the pigment mixtures discussed in the present research (lead white and cinnabar, and lead white and azurite). This approach ensures that the pXRF technique can effectively identify key pigment elements, even when they are unevenly distributed and mixed in varying concentrations, as is the case in real paintings.

The specific area chosen for Case Study No.1, which involves the painting *Boceto di Pablo Veronese*, was the red colour (points 1, 2, 27, 28) and flesh tone (points 3, 4, 5, 12, 14, 16, 17, 19, 24) (Figure 10a).

The identification of the chemical elements and the composition of the crystalline pigments in these areas (cinnabar, cerussite and hydrocerussite) was carried out by our research group [2] by using pXRF and XRD on measurements taken directly from the surface of the painting. The combined data from XRD results, the cinnabar map, and the XRF peaks such as Hg and Pb observed in the spectrum of Figure 11a, supported the findings of our study on laboratory samples.

Figure 10. Areas chosen for: *a)* Case Study No. 1: painting on copper support and *b)* for Case Study No. 2: painting on canvas.

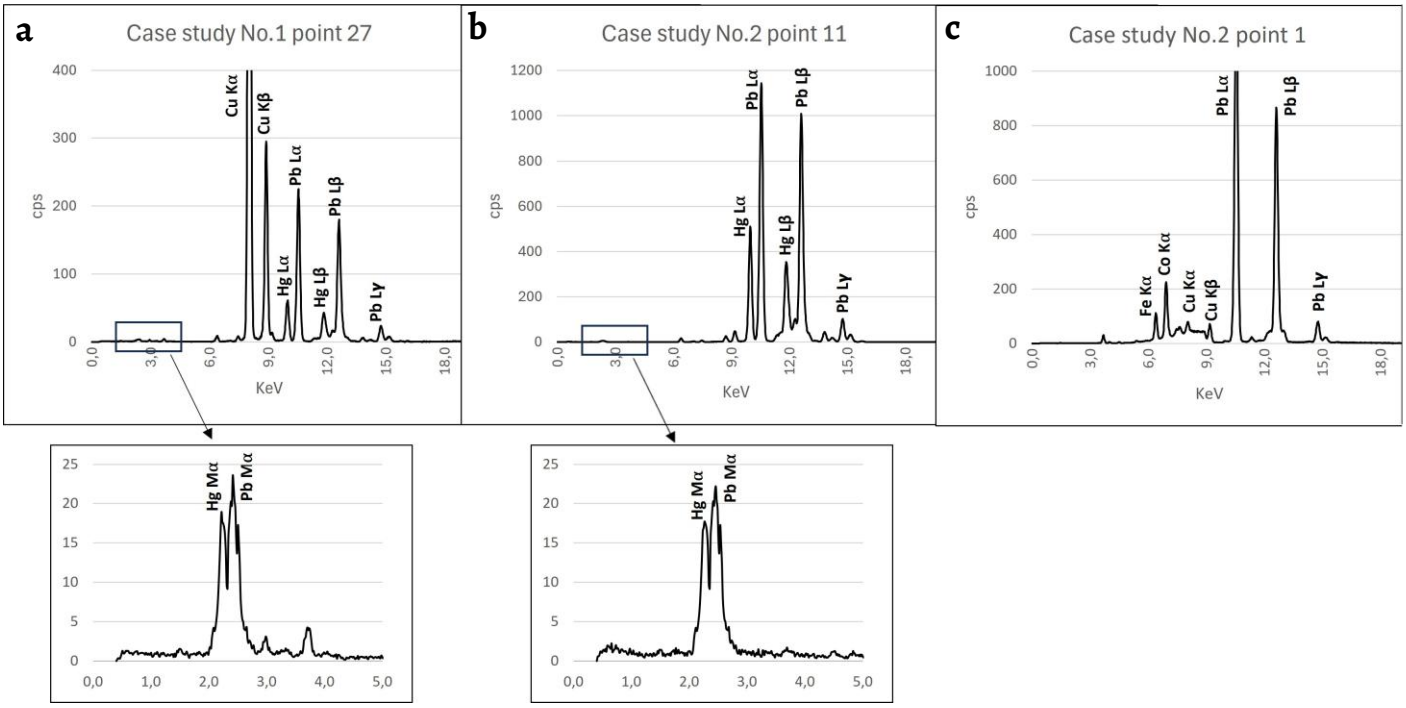

Figure 11. pXRF spectra corresponding to the following areas: *a)* Case study No.1: Point 27; *b)* Case study No.2 point 11; *c)* Case study No.2 point 1.

Table 1. Elements identified via pXRF associated with the ground and pictorial layers of the painting on canvas (case study No. 2). (M) major, (m) minor and (tr) trace elements.

Color	No.	Elements detected				
		Pb	Cu	Hg	Fe	Co
Blue	1	M	M	-	M	M
	2	M	M	-	M	M
	3	M	M	-	M	M
	4	M	M	-	M	M
	5	M	M	-	M	M
	6	M	M	-	M	M
Red	7	M	-	M	m	-
	8	M	-	M	M	-
	9	M	-	M	m	-
	10	M	-	M	m	-
	11	M	-	M	m	-
	12	M	-	M	M	-
	13	M	-	M	M	-
Flesh tone	14	M	-	m	tr	-
	15	M	-	M	tr	-
	16	M	-	M	tr	-
	17	M	-	tr	tr	-
	18	M	-	tr	tr	-
	19	M	-	tr	M	-
	20	M	-	m	tr	-
	21	M	-	tr	tr	-
	22	M	-	m	tr	-
	23	M	-	tr	tr	-

The areas selected for Case Study No. 2 (*The Little Madonna of Foligno*) include the blue, red, and flesh tones (Figure 10b). The results of the pXRF analysis are presented in Table 1, with selected spectra shown in Figure 11b-c. Pb and Hg were identified in the red area (points 7-13), attributed to vermilion or cinnabar (HgS); Pb and Cu in the blue area (points 1-6) attributed to azurite and lead white pigments ($Cu_3(CO_3)_2(OH)_2$ and $(PbCO_3)_2{\cdot}Pb(OH)_2$), and Pb and Hg, with traces of Fe, in the flesh-coloured area (points 14-23) attributed to vermilion or cinnabar and lead white. These findings were corroborated using XRD results previously published by our research team [29], which identified cinnabar, cerussite, hydrocerussite, and azurite.

Additionally, as seen in Figure 11a-b, the peaks corresponding to the spectral lines HgMα and PbMα are present. As described in *Stratigraphical information obtained* section, their presence suggests that cinnabar and lead white pigments are located in the external layers.

Discussion

pXRF spectra from the samples analysed showed well-defined peaks without overlapping. However, the results showed that the matrix effect does indeed play a crucial role in the detection of pigments from complex multilayer samples using pXRF, because it can either enhance or attenuate the signal of an element in a pigment, depending on the surrounding materials and their composition. These effects occurred because both the analyte and the matrix can absorb and fluoresce in the X-ray region, which in turn affected the magnitude of the analyte signal.

The X-ray fluorescence signal decreased more when the analysed pigment was in the inner layer (up to 90 % in some cases, such as CuKα), and the signal of the pigment in the outer layer decreased because of the nature of the pigments in the lower layers (up to 50 %). The attenuation of X-rays was justified since the X-rays produced in the fluorescence process are generated both in the atoms on the surface of the sample and in those within the sample. When a beam of X-ray photons passes through a material, some photons are attenuated in the interaction processes, reflecting the Beer-Lambert law. The intensity of both the incident X-ray beam and the fluorescent radiation is reduced due to absorption in the sample, which depends on the density, thickness, and mass attenuation coefficient of all the elements in the matrix. For samples of similar density and thickness, as in our experimental replica samples, the attenuation will depend mainly on the attenuation coefficient of the different elements that make up the sample, which in turn depends on the types of atoms present and the energy of the interacting photons. If the top layer contains a pigment containing a heavy element, like Hg in the case of cinnabar, this can absorb the X-rays emitted by a lighter element in another pigment from a lower layer, like azurite, reducing the signal of this latter pigment.

A significant reduction was observed in the X-ray fluorescence signals for HgLα, CuKα, CdKα, and PbLα in binary, ternary, and quaternary mixtures (more than 50 % in all mixtures, reaching 95 % in the quaternary mixture). The X-ray fluorescence signals of each pigment in quaternary mixtures become so weak that it was difficult to detect individual pigments. The Pb signal in binary mixtures with azurite or cadmium yellow is barely modified (40 %), but with cinnabar, the influence of Hg on the X-ray fluorescence measurement of Pb was clear (75 %). The presence of lead white significantly affected the fluorescence signals of other pigments in the mixture, with varying degrees of impact depending on the particular pigment and the ratio used in the mixture (up to 80 %). If the pigments are not only mixed but are distributed in multilayers, the decrease in the X-ray fluorescence signal is greater than if they were pure pigments in multilayers.

On the other hand, the so-called enhancement effect caused by elements in the matrix is also observed, leading to higher-than-expected results. It occurs when the radiation from another element in the matrix causes a secondary excitation, one associated with an element with a higher atomic number than that of the fluorescent element [33]. Thus, when Cd and Hg

are measured together, that is, submitted to the same incident radiation, both elements are excited by the primary radiation, and the Cd atoms are also subjected to the Hg fluorescent radiation, which is sufficiently energetic to expel an inner electron of Cd atoms. This causes an increase in intensity over and above that due to the primary excitation, and an additional Cd emission is observed.

Finally, the results confirm that we can ascertain whether pigments with elements such as Pb, Cd and Hg are found in a surface layer or in an internal layer by reference to the spectral lines obtained in the XRF spectrum, independently of whether the pigments are pure or mixed. X-ray fluorescence (pXRF) spectrometry can thus be regarded as a well-established bulk analytical technique for assessing the total content of several chemical elements in many different types of samples.

Despite the detected signal being influenced by the sample's composition and geometry as described by the Beer-Lambert law, portable X-ray fluorescence remains a powerful tool for detecting and identifying elements in the studied pigments, even in complex or layered structures. The ability of pXRF to provide in situ, detailed elemental analysis without damaging the sample makes it particularly valuable in fields like art restoration and conservation.

Conclusions

The present research explores the challenges of using portable X-ray fluorescence analysis (pXRF) to detect, in situ, specific pigments like azurite, cinnabar, cadmium yellow, and lead white in complex stratigraphic layers and mixtures, as is typically found in historical paintings and polychrome sculptures. The research highlights how the intensity of the X-ray fluorescence radiation from elements like HgLα for cinnabar, CuKα for azurite, CdKα for cadmium yellow and PbLα for lead white can be affected in these complex stratigraphic structures. But pXRF analysis can identify the pigments in situ in a non-invasive manner, determining whether pigments with Pb, Hg or Cd are found in superficial layers or in internal layers. The findings from the experimental replica samples studied were applicated in two real paintings used as case study, where the pigments (cinnabar, lead white and azurite) are in-homogeneously distributed and mixed in different concentrations. It can be concluded that in real paintings, the matrix effect on the measurement of the fluorescence signal does not prevent the identification of the key elements of these pigments by means of hand-held XRF instrumentation for in situ measurements. Furthermore, in real paintings, it has been possible to identify whether those containing Pb, Hg, and Cd are located at the surface level or in an internal layer.

Acknowledgements
We thank the research group FQM-338.

Data availability statement

The data presented in this study are available on request from the corresponding author.

REFERENCES

1. West, M.; Ellis, A.T.; Potts, P. J.; Streli, C.; Vanhoof, C.; Wobrauschek, P., 'Atomic spectrometry update – a review of advances in X-ray fluorescence spectrometry and their applications', *Journal of Analytical Atomic Spectrometry* **30**(9) (2015) 1839-1889, https://doi.org/10.1039/C5JA90033F.
2. Blanc, R.; Manzano, E.; López-Montes, A.; Domínguez-Gasca, N.; Vílchez, J.L., 'Non-invasive study of the pigments of a painting on copper with the inscription "Boceto di Pablo Veronese" on the back', *Heritage* **6**(6) (2023) 4787-4801, https://doi.org/10.3390/heritage6060254.

3. Leutenegger, P.; Longoni, A.; Fiorini, C.; Strüder, L.; Kemmer, J.; Lechner, P.; Cesareo, R., 'Works of art investigation with silicon drift detectors', *Nuclear Instruments and Methods in Physics Research Section A* **439**(2-3) (2000) 458-470, https://doi.org/10.1016/S0168-9002(99)00908-0.
4. Ferrero, J. L.; Roldan, C.; Ardid, M.; Navarro, E., 'X-ray fluorescence analysis of yellow pigments in altarpieces by Valencian artists of the XV and XVI centuries', *Nuclear Instruments and Methods in Physics Research Section A* **422**(1-3) (1999) 868-873, https://doi.org/10.1016/S0168-9002(98)01125-5.
5. Orsilli, J.; Caglio S., 'Combined scanned macro X-ray fluorescence and reflectance spectroscopy mapping on corroded ancient bronzes', *Minerals* **14**(2) (2024) 192-205, https://doi.org/10.3390/min14020192.
6. Alberghina, M. F.; Zicarelli, M. A.; Randazzo, L.; Schiavone, S.; La Russa, M. F.; Labriola, M.; Ricca, M., 'Byzantine wall paintings from San Marco d'Alunzio, Sicily: non-invasive diagnostics and microanalytical investigation of pigments and plasters', *Heritage Science* **12**(1) (2024) 184-201, https://doi.org/10.1186/s40494-024-01308-z.
7. Harth, A., 'X-ray fluorescence (XRF) on painted heritage objects: a review using topic modeling', *Heritage Science* **12**(1) (2024) 17-29, https://doi.org/10.1186/s40494-024-01135-2.
8. Bonizzoni, L.; Colombo, C.; Ferrati, S.; Gargano, M.; Greco, M.; Ludwig, N.; Realini, M., 'A critical analysis of the application of EDXRF spectrometry on complex stratigraphies', *X-Ray Spectrometry* **40**(4) (2011) 247-253, https://doi.org/10.1002/xrs.1320.
9. Tykot, R., 'Using non-destructive portable X-ray fluorescence spectrometers on stone, ceramics, metals, and other materials in museums: advantages and limitations', *Applied Spectroscopy* **70**(1) (2016) 42-56, https://doi.org/10.1177/0003702815616745.
10. Shugar, A. N.; Mass, J. L., *Handheld XRF for art and archaeology*, Leuven University Press, Leuven (2012).
11. Sugihara, K.; Tamura, K.; Satoh, M.; Hayakawa, Y.; Hirao, Y.; Miura, S.; Tokugawa, Y., 'Analysis of pigments used in scroll paintings of a national treasure "Tale of Genji" using a portable x-ray fluorescence spectrometer', *Advances in X-ray Analysis* **44** (2001) 432-441.
12. Bettinelli, M.; Taina, P., 'Rapid analysis of coal fly ash by x-ray fluorescence spectrometry', *X-Ray Spectrometry* **19**(5) (1990) 227-232, https://doi.org/10.1002/xrs.1300190505.
13. Ferrero, J. L.; Roldán, C.; Juanes, D.; Rollano, E.; Morera, C., 'Analysis of pigments from Spanish works of art using a portable EDXRF spectrometer', *X-Ray Spectrom*etry **31**(6) (2002) 441-447, https://doi.org/10.1002/xrs.604.
14. Frahm; E., Doonan, R.C., 'The technological versus methodological revolution of portable XRF in archaeology', *Journal of Archaeological Science* **40**(2) (2013) 1425-1434, https://doi.org/10.1016/j.jas.2012.10.013.
15. Galli, A.; Bonizzoni, L., 'True versus forged in the cultural heritage materials: the role of analysis', *X-Ray Spectrometry* **43**(1) (2014) 22-28, https://doi.org/10.1002/xrs.2461.
16. Manhas, M.; Tomar, A.; Tiwari, M.; Sharma, S., 'Application of X-ray fluorescence in forensic archaeology: a review', *X-Ray Spectrometry* **54**(1) (2025) 26-37, https://doi.org/10.1002/xrs.3421.
17. Fontana, D.; Alberghina, M. F.; Barraco, R.; Basile, S.; Tranchina, L.; Brai, M.; Troja, S. O., 'Historical pigments characterisation by quantitative X-ray fluorescence', *Journal of Cultural Heritage* **15**(3) (2014) 266-274, https://doi.org/10.1016/j.culher.2013.07.001.
18. Shibata, Y.; Suyama, J.; Kitano, M.; Nakamura, T., 'X-ray fluorescence analysis of Cr, As, Se, Cd, Hg, and Pb in soil using pressed powder pellet and loose powder methods', *X-Ray Spectrometry* **38**(5) (2009) 410-416, https://doi.org/10.1002/xrs.1195.
19. Narman Han, E.; Boydaş, E., 'Characterization of matrix effects for Pb L-shell energy dispersive X-ray fluorescence (EDXRF) in binary compounds of cadmium, copper, molybdenum, and zinc', *Instrumentation Science & Technology* **49**(6) (2021) 616-62, https://doi.org/10.1080/10739149.2021.1923029.
20. Bonizzoni, L., 'ED-XRF analysis for cultural heritage: is quantitative evaluation always essential?', *Journal of Physics Conference Series* **630**(1) (2015) 012001, https://doi.org/10.1088/1742-6596/630/1/012001.
21. Mantler, M.; Schreiner, M., 'X-ray fluorescence spectrometry in art and archaeology', *X-Ray Spectrometry* **29**(1) (2000) 3-17, https://doi.org/10.1002/(SICI)1097-4539(200001/02)29:1%3C3::AID-XRS398%3E3.0.CO;2-O.
22. De Viguerie, L.; Sole, V. A.; Walter, P., 'Multilayers quantitative X-ray fluorescence analysis applied to easel paintings', *Analytical and Bioanalytical Chemistry* **395** (2009) 2015-2020, https://doi.org/10.1007/s00216-009-2997-0.
23. Bonizzoni, L.; Galli, A.; Milazzo, M., 'XRF analysis without sampling of Etruscan depurata pottery for provenance classification', *X-Ray Spectrometry* **39**(5) (2010) 346-352, https://doi.org/10.1002/xrs.1263.
24. Giurlani, W.; Berretti, E.; Lavacchi, A.; Innocenti, M., 'Thickness determination of metal multilayers by ED-XRF multivariate analysis using Monte Carlo simulated standards', *Analitica Chimica Acta* **1130** (2020) 72-79, https://doi.org/10.1016/j.aca.2020.07.047.
25. Pessanha, S.; Guilherme, A.; Carvalho, M. L., 'Comparison of matrix effects on portable and stationary XRF spectrometers for cultural heritage samples', *Applied Physics A* **97** (2009) 497-505, https://doi.org/10.1007/s00339-009-5251-x.
26. Manzano, E.; Blanc, R.; Martin-Ramos, J. D.; Chiari, G.; Sarrazin, P.; Vilchez, J. L., 'A combination of invasive and non-invasive techniques for the study of the palette and painting structure of a copy of Raphael's Transfiguration of Christ', *Heritage Science* **9** (2021) 150, https://doi.org/10.1186/s40494-021-00623-z.
27. Cesareo, R.; De Assis, J. T.; Roldán, C.; Bustamante, A. D.; Brunetti, A.; Schiavon, N., 'Multilayered samples reconstructed by measuring Kα/Kβ or Lα/Lβ X-ray intensity ratios by EDXRF', *Nuclear Instruments and Methods in Physics Research Section B* **312** (2013) 15-22, https://doi.org/10.1016/j.nimb.2013.06.019.
28. Karimi, M.; Amiri, N.; Tabbakh Shabani, A. A., 'Thickness measurement of coated Ni on brass plate using Kα/Kβ ratio by XRF spectrometry', *X-Ray Spectrometry* **38**(3) (2009) 234-238, https://doi.org/10.1002/xrs.1146.

29. Martín-Ramos, J. D.; Zafra-Gómez, A.; Vílchez, J. L., 'Non-destructive pigment characterization in the painting Little Madonna of Foligno by X-ray powder diffraction', *Microchemical Journal* **134** (2017) 343-353, https://doi.org/10.1016/j.microc.2017.07.001.
30. Feller, R. L., *Artists' pigments: a handbook of their history and characteristics*, vol. 47, National Gallery of Art, Washington (1986).
31. Mosca, S.; Frizzi, T.; Pontone, M.; Alberti, R.; Bombelli, L.; Capogrosso, V.; Nevin, A.; Valentini, G.; Comelli, D., 'Identification of pigments in different layers of illuminated manuscripts by X-ray fluorescence mapping and Raman spectroscopy', *Microchemical Journal* **124** (2016) 775-784, https://doi.org/10.1016/j.microc.2015.10.038.
32. Ruberto, C.; Mazzinghi, A.; Massi, M.; Castelli, L.; Czelusniak, C.; Palla, L.; Gelli N.; Betuzzi, M.; Impallaria, A.; Brancaccio, R.; Peccenini, E.; Raffaelli, M., 'Imaging study of Raffaello's "La Muta" by a portable XRF spectrometer', *Microchemical Journal* **126** (2016) 63-69, https://doi.org/10.1016/j.microc.2015.11.037.
33. Shackley, M. S., 'An introduction to X-Ray fluorescence (XRF) analysis in archaeology', *X-ray fluorescence spectrometry (XRF) in geoarchaeology*, ed. M. S. Shackley, Springer, New York (2012) 18-24.

RECEIVED: 2025.6.5
REVISED: 2025.11.13
ACCEPTED: 2025.12.8
ONLINE: 2026.6.2